

Adsorbed Gas Layers Limit the Mobility of Micropancakes

Teshima, Hideaki

Department of Aeronautics and Astronautics, Kyushu University

Takata, Yasuyuki

International Institute for Carbon-Neutral Energy Research (WPI-I2CNER), Kyushu University

Takahashi, Koji

Department of Aeronautics and Astronautics, Kyushu University

<https://hdl.handle.net/2324/4793639>

出版情報 : Applied Physics Letters. 115 (7), pp.071603-, 2019-08-14. American Institute of Physics : AIP

バージョン :

権利関係 : ©2019 Author(s).



Adsorbed gas layers limit the mobility of micropancakes

Cite as: Appl. Phys. Lett. **115**, 071603 (2019); <https://doi.org/10.1063/1.5113810>

Submitted: 07 June 2019 • Accepted: 25 July 2019 • Published Online: 14 August 2019

Hideaki Teshima, Yasuyuki Takata and Koji Takahashi



View Online



Export Citation



CrossMark

ARTICLES YOU MAY BE INTERESTED IN

[Wettability of AFM tip influences the profile of interfacial nanobubbles](#)

Journal of Applied Physics **123**, 054303 (2018); <https://doi.org/10.1063/1.5010131>

[Nanoscale pinning effect evaluated from deformed nanobubbles](#)

The Journal of Chemical Physics **146**, 014708 (2017); <https://doi.org/10.1063/1.4973385>

[Nanobubbles on solid surface imaged by atomic force microscopy](#)

Journal of Vacuum Science & Technology B: Microelectronics and Nanometer Structures Processing, Measurement, and Phenomena **18**, 2573 (2000); <https://doi.org/10.1116/1.1289925>

 QBLOX



1 qubit

Shorten Setup Time

Auto-Calibration

More Qubits

Fully-integrated

Quantum Control Stacks

Ultrastable DC to 18.5 GHz

Synchronized <<1 ns

Ultralow noise



100s qubits

[visit our website >](#)

Adsorbed gas layers limit the mobility of micropancakes

Cite as: Appl. Phys. Lett. **115**, 071603 (2019); doi: [10.1063/1.5113810](https://doi.org/10.1063/1.5113810)

Submitted: 7 June 2019 · Accepted: 25 July 2019 ·

Published Online: 14 August 2019



View Online



Export Citation



CrossMark

Hideaki Teshima,^{1,2} Yasuyuki Takata,^{2,3} and Koji Takahashi^{1,2,a)}

AFFILIATIONS

¹Department of Aeronautics and Astronautics, Kyushu University, Nishi-Ku, Motooka 744, Fukuoka 819-0395, Japan

²International Institute for Carbon-Neutral Energy Research (WPI-I2CNER), Kyushu University, Nishi-Ku, Motooka 744, Fukuoka 819-0395, Japan

³Department of Mechanical Engineering, Kyushu University, Nishi-Ku, Motooka 744, Fukuoka 819-0395, Japan

^{a)}Author to whom correspondence should be addressed: takahashi@aero.kyushu-u.ac.jp

ABSTRACT

In contrast to surface nanobubbles, the properties of atomically flat gas phases such as micropancakes remain unclear. In this study, we investigated nanoscopic gas phases existing at the interface between highly ordered pyrolytic graphite and air-supersaturated pure water using high-sensitivity frequency-modulation atomic force microscopy (AFM). Micropancakes appeared on a disordered gas layer overlying an ordered gas layer and moved in the direction of AFM scanning. Their movement stopped at the edge of the disordered gas layers, whereas the two gas layers did not move at all. The limited mobility of micropancakes is explained by assuming that the disordered and ordered gas layers, which are composed of strongly adsorbed gas molecules, behave like solid surfaces, and that the surface heterogeneity between them results in a pinning effect.

Published under license by AIP Publishing. <https://doi.org/10.1063/1.5113810>

Nanoscale gaseous phases that exist at the solid/liquid interface were first observed in 2000^{1,2} and have since attracted increasing attention for a wide range of engineering applications, such as wafer-scale transfer of graphene films³ and nucleate boiling with low superheat.⁴ However, to adopt surface nanobubbles in such applications, further understanding of their properties based on detailed observations is necessary. To date, three imaging methods have been used to image surface nanobubbles: optical microscopy,^{5–7} transmission electron microscopy,^{8–10} and atomic force microscopy (AFM).^{11–17} Each of these methods has advantages and disadvantages and thus should be used according to the specific experimental aims. Of these methods, AFM has been the most widely used technique for surface nanobubbles. The reason for this is that AFM can provide the 3D profile of surface nanobubbles, which is essential for understanding their properties, such as large contact angles,¹ long-lifetime,^{11,12} shape transformations from a 2D gas structure to a spherical-cap form,^{13–15} and strong pinning of their three-phase contact line.^{11,16} These studies have greatly contributed to the development of the theory describing surface nanobubbles.¹⁷

The first AFM observation of surface nanobubbles was conducted in the amplitude-modulation (AM) mode.^{1,2} Since then, it has become widely recognized that two types of gas phases exist at the solid/liquid interface: Spherical cap-shaped nanobubbles^{1,11,12,14–16,18,19} and

micropancakes.^{13–15,18,20–23} Various theories have been proposed to describe these gas phases.^{24–29} Moreover, theories have been developed that consider not only the properties of these states but also related interfacial phenomena, such as the reduction of surface drag of fluids³⁰ and the long-range attraction force between hydrophobic surfaces.³¹

Recently, more-detailed observations of interfacial gas phases have been enabled by advanced AFM modes, namely, peak-force quantitative nanomechanical mapping,^{14,16,19,32–35} high-speed scanning AM mode,¹⁵ and frequency-modulation (FM) mode.^{14,18,36,37} These studies have revealed the existence of novel interfacial gas phases, such as a circular fluid layer,¹⁴ an ordered epitaxial layer,^{14,18,36,37} a disordered layer,¹⁸ and mobile micropancakes.¹⁵ These findings indicate that the phenomena of interfacial nanoscale gas phases are more complex than expected, thus necessitating more in-depth analysis. However, such advanced AFM studies are rare, with FM mode measurements only having been reported by Hwang's group.^{14,18,36,37} In the present study, we observed a highly ordered pyrolytic graphite (HOPG)/pure water interface using FM-AFM and found that mobile micropancakes sit on a disordered gas layer. We present a mechanism to explain their mobility.

We used the FM mode of an SPM-8100FM AFM (Shimadzu Corp.), which can achieve higher sensitivity than imaging in the normal tapping mode or peak-force tapping mode. This mode oscillates

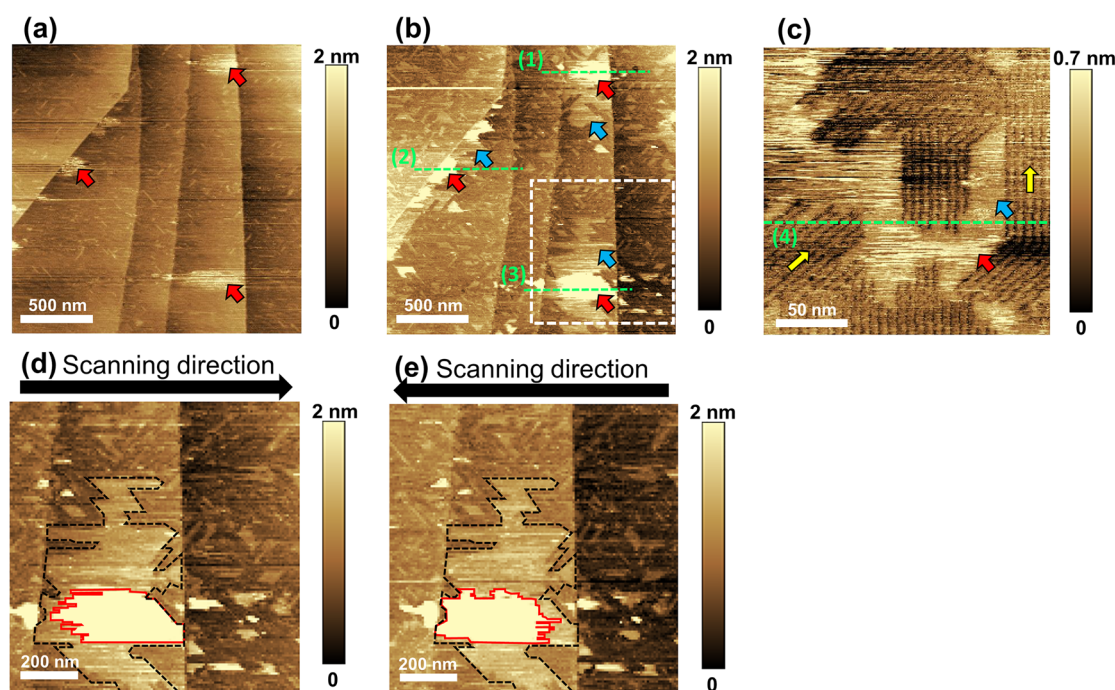


FIG. 1. (a) and (b) Height images ($2\ \mu\text{m} \times 2\ \mu\text{m}$) of the HOPG/pure water interface obtained with cantilever peak-to-peak oscillation amplitudes of approximately 4 and 0.8 nm, respectively. The red arrows indicate micropancakes, and the blue arrows indicate disordered gas layers. (c) Higher resolution height image ($200\ \text{nm} \times 200\ \text{nm}$) of nanoscopic gas phases. The yellow arrows indicate the direction of ordered gas molecules. The height profiles measured along the green broken lines (1–4) are shown in the [supplementary material](#) [Fig. S1(1–4)]. (d) and (e) Magnified images of a micropancake on a disordered gas layer in the area surrounded by a white broken line in (b). The image in (d) was obtained by scanning data from the left side to the right side (i.e., a trace image) and (e) was obtained by scanning in the opposite direction (i.e., a retrace image). The red line indicates the shape of the micropancake. The black broken line indicates the edge of the disordered gas layer.

the cantilever at its resonance frequency, which slightly shifts to a positive value when a repulsive force is applied, and utilizes the magnitude of the shift as a feedback parameter. In this experiment, the frequency shift of the AFM cantilever while moving across the sample surface was set to +83 Hz. A PPP-NCHR cantilever (Nanosensors) with a tip radius of $\sim 10\ \text{nm}$ was used, and its spring constant, calibrated by Sader's method,³⁸ was 54.5 N/m. The resonance frequency of the cantilever in the liquid was 163 kHz. Because it is desirable to use a hydrophilic tip³² for detecting gas phases in the liquid, we treated the cantilever with oxygen plasma (Plasma Reactor 500, Yamato Scientific, Japan) for 30 min. The height data were captured with a resolution of 256 pixels \times 256 pixels and scan rates of 0.5 or 0.3 Hz.

HOPG (SPI-1 grade, 10 mm \times 10 mm, Alliance Biosystems, Inc., Japan) was used as the substrate surface. Gas phases were generated on the surface through the solvent-exchange method¹ using air-saturated pure water and ethanol. When adding solvents, a clean glass syringe and steel needle were used to avoid contamination from the silicone oil.³⁹

Two height images of an HOPG surface in water using different cantilever oscillation amplitudes are shown in Figs. 1(a) and 1(b). The two images exhibit clear differences, although the scan areas were the same for both. In Fig. 1(a), which was obtained with an amplitude of 4 nm, there are HOPG step structures with heights of about 0.3–0.6 nm (i.e., one- or two-atom thickness) and bright regions indicated by red arrows with heights of $\sim 1.5\ \text{nm}$. By contrast, in Fig. 1(b),

which was obtained with an amplitude of 0.8 nm, the bright regions became larger (height: $\sim 5\ \text{nm}$). These thick regions have a flat shape [see Fig. S1(1–3)] similar to the micropancakes reported in previous studies.^{13,15,18,20–23} In addition, many thin layers with heights of 0.3–0.5 nm, indicated by blue arrows, were found on the surface. In the high-resolution image of an HOPG/pure water interface [Fig. 1(c)], we found that there were rowlike structures around the thin layers, as indicated by the yellow arrows and the absence of a bare HOPG surface. These rowlike structures are likely to be caused by the six-membered ring structure of the underlying HOPG surface. This is consistent with reports from Hwang's group that these structures are epitaxially grown ordered gas layers.^{14,18,36,37} By contrast, the thin gas layers were slightly higher than the ordered gas layers [see Fig. S1(4)] and did not exhibit a rowlike structure; thus, it can be considered that they were disordered gas layers nucleated on the ordered gas layers.¹⁸

Imaging with a small amplitude enables us to observe the gas phases accurately, as can be seen from the comparison of Figs. 1(a) and 1(b), for two reasons. One is the increase in imaging sensitivity. A smaller amplitude increases the interaction time between the AFM tip and the sample surface, because the interaction distance of the repulsive van der Waals force is very short (typically less than 0.5 nm). This improves the signal-to-noise ratio, resulting in high-sensitivity imaging.^{40,41} It was also reported that in the normal tapping mode, which is less sensitive than the FM mode, ordered gas layers cannot be observed.³⁷ The second reason is the decrease in the load force of the cantilever tip on the sample

surface. The load force can be estimated using Sader's formula.⁴² In Fig. 1(a), which was obtained with an amplitude of 4.0 nm, the applied repulsive force corresponding to the frequency shift of +83 Hz was approximately 830 pN. This large force squashes the surface nanobubbles and leads to underestimation of their height.^{34,35} By contrast, in Fig. 1(b), the load force when the amplitude was 0.8 nm decreased to approximately 70 pN, which is considerably smaller than the typical values used in some nanobubble measurements^{14,16,19,32–35} and enables us to capture the interfacial gas phases more accurately.

Figures 1(d) and 1(e) show the trace and retrace images of the area indicated by the white square in Fig. 1(b). These images were simultaneously obtained during the measurement. Micropancakes, indicated by red lines, moved in the scanning direction. Furthermore, micropancake movement was limited by the edges of the disordered gas layer, which are indicated by the black broken line. This result suggests that mobile micropancakes are located on the disordered gas layers and do not sit on the HOPG surface directly. As indicated by the black broken lines, the disordered gas layer did not change its shape between Figs. 1(d) and 1(e), even as the micropancake moved on it. We also confirmed that the ordered gas layer did not change its shape owing to the movement of the AFM tip. We conclude that the gas molecules constituting the ordered and disordered gas layers are strongly adsorbed on the graphite surface and do not easily depart from the surface. All micropancakes and ordered gas layers observed in our experiments exhibited the same characteristics.

We have investigated HOPG/pure water interfaces by FM-AFM ten times, with the same conditions as mentioned in this study. As a result, we found adsorbed gas layers every time and micropancakes five times out of ten times, while spherical-cap shaped nanobubbles were found only one time. This difference might be caused by the difference in the local gas concentration at the HOPG/pure water interface.⁴³ This parameter cannot be precisely controlled using the solvent exchange method.

To explain why micropancakes move on the underlying disordered gas layer and stop at the boundary of the disordered gas layers, we propose the following mechanism of generation of interfacial gas structures. First, as illustrated in Fig. 2(a), excess gas molecules appeared during solvent exchange and adhered to the HOPG surface. This is consistent with a previous experimental observation that adhesion of gas molecules occurs, even in the degassed water.³⁷ The interaction potential at the gas/solid interface is typically an order of magnitude stronger than that at the gas/gas interface.¹⁸ Therefore, as depicted in Fig. 2(b), the gas molecules adsorbed to the HOPG surface behave as solid surfaces. The gas molecules closest to the HOPG surface are strongly affected by the surface's crystalline structure and thus exhibit an ordered structure. By contrast, the gas molecules adhered to the ordered gas layers become a solidlike but disordered layer. This is because the ordered gas layer creates a space between the disordered layer and the underlying HOPG surface, and thus, the interaction between them becomes weak. Furthermore, the gas molecules aggregated on the disordered layer form micropancakes, which move on the underlying disordered gas layer in the direction of the AFM tip owing to the weaker interaction. In addition, chemical and/or geometrical heterogeneities should exist between the different solid surfaces, resulting in a pinning effect. Therefore, as illustrated in Fig. 2(c), the micropancakes are pinned at the boundary between the solidlike disordered gas layer and the underlying ordered gas layer.

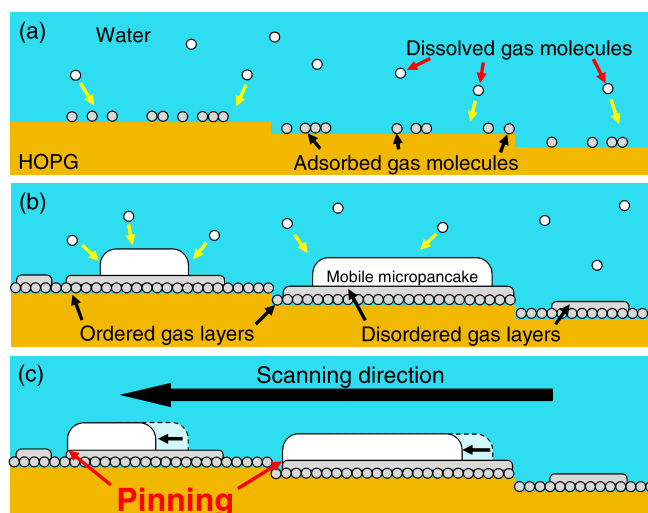


FIG. 2. Proposed mechanism for the generation of two adsorbed gas layers and mobile micropancakes. (a) Adsorption of dissolved gas molecules. Dissolved and adsorbed gas molecules are indicated by white and gray circles, respectively. (b) Nucleation of micropancakes on solidlike disordered gas layers. (c) Pinning of mobile micropancakes at the boundary between the disordered gas layers and ordered layers. Some structures are not represented to scale for clarity.

Finally, we confirmed that the mobile micropancakes are indeed gas phases and not contaminants. In Figs. 3(a) and 3(b), several mobile micropancakes (bright regions) were found, which appeared to move in the scanning direction. After imaging, we added degassed water to the liquid cell and scanned the same area again [Fig. 3(c)]. As a result, some micropancakes disappeared, as indicated by the green circles. This result confirms that these micropancakes were a gas phase (i.e., not an insoluble contaminant³⁹) and dissolved in the water owing to the reduction of the gas concentration.

Almost all previously reported micropancakes were found to be immobile and did not move as a result of tip movement.^{13,20–22} Only one report claimed that micropancakes can migrate because of tip movement.¹⁵ However, the relationship between mobile micropancakes and adsorbed gas layers remained veiled until our FM-AFM measurements of mobile micropancakes sitting on disordered gas layers. Specifically, we observed that their mobility was limited by the underlying adsorbed gas layers. We explained this phenomenon by assuming that strongly adsorbed gas molecules behave as solidlike gas

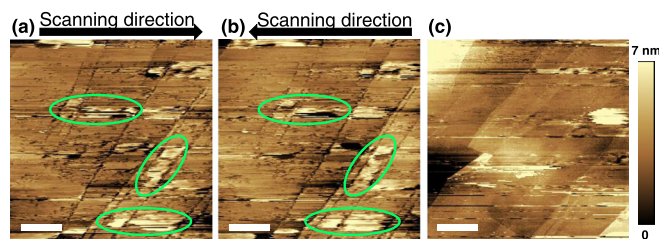


FIG. 3. Height images ($5\ \mu\text{m} \times 5\ \mu\text{m}$) of the HOPG/pure water interface (a) and (b) before and (c) after adding degassed water. Panels (a) and (b) show the trace and retrace images, respectively. The green circles indicate that mobile micropancakes disappeared in image (c). The scale bars are $1\ \mu\text{m}$.

layers, resulting in chemical and/or geometrical heterogeneity and thus a pinning effect. These results extend our knowledge not only about micropancakes but also about the dynamics of gas molecules at solid/liquid interfaces.

See the [supplementary material](#) for the height profiles of interfacial gas phases shown in [Figs. 1\(b\) and 1\(c\)](#).

This work was partially supported by JST CREST Grant No. JPMJCR18I1, JSPS KAKENHI Grant No. JP17H03186, a Grant-in-Aid for JSPS Research Fellow No. JP18J11880, and a project commissioned by the New Energy and Industrial Technology Development Organization (NEDO), Japan. We thank Dr. Takashi Nishiyama, Mr. Tatsuya Ikuta, and Mr. Naoto Nakamura for their discussion about the behavior of micropancakes and experimental help.

REFERENCES

- ¹S.-T. Lou, Z.-Q. Ouyang, Y. Zhang, X.-J. Li, J. Hu, M.-Q. Li, and F.-J. Yang, *J. Vac. Sci. Technol., B* **18**, 2573 (2000).
- ²N. Ishida, T. Inoue, M. Miyahara, and K. Higashitani, *Langmuir* **16**, 6377 (2000).
- ³L. Gao, G. X. Ni, Y. Liu, B. Liu, A. H. Castro Neto, and K. P. Loh, *Nature* **505**, 190 (2014).
- ⁴Y. Nam and Y. S. Ju, *Appl. Phys. Lett.* **93**, 103115 (2008).
- ⁵X. Zhang, H. Lhuissier, C. Sun, and D. Lohse, *Phys. Rev. Lett.* **112**, 144503 (2014).
- ⁶B. H. Tan, H. An, and C.-D. Ohl, *Phys. Rev. Lett.* **118**, 054501 (2017).
- ⁷C. U. Chan and C.-D. Ohl, *Phys. Rev. Lett.* **109**, 174501 (2012).
- ⁸Y. Tomo, K. Takahashi, T. Nishiyama, T. Ikuta, and Y. Takata, *Int. J. Heat Mass Transfer* **108**, 1460 (2017).
- ⁹D. Shin, J. B. Park, Y.-J. Kim, S. J. Kim, J. H. Kang, B. Lee, S.-P. Cho, B. H. Hong, and K. S. Novoselov, *Nat. Commun.* **6**, 6068 (2015).
- ¹⁰J. B. Park, D. Shin, S. Kang, S.-P. Cho, and B. H. Hong, *Langmuir* **32**, 11303 (2016).
- ¹¹X. Zhang, D. Y. C. Chan, D. Wang, and N. Maeda, *Langmuir* **29**, 1017 (2013).
- ¹²X. H. Zhang, A. Quinn, and W. A. Ducker, *Langmuir* **24**, 4756 (2008).
- ¹³L. Zhang, X. Zhang, C. Fan, Y. Zhang, and J. Hu, *Langmuir* **25**, 8860 (2009).
- ¹⁴C.-K. Fang, H.-C. Ko, C.-W. Yang, Y.-H. Lu, and I.-S. Hwang, *Sci. Rep.* **6**, 24651 (2016).
- ¹⁵H.-S. Liao, C.-W. Yang, H.-C. Ko, E.-T. Hwu, and I.-S. Hwang, *Appl. Surf. Sci.* **434**, 913 (2018).
- ¹⁶H. Teshima, T. Nishiyama, and K. Takahashi, *J. Chem. Phys.* **146**, 014708 (2017).
- ¹⁷D. Lohse and X. Zhang, *Rev. Mod. Phys.* **87**, 981 (2015).
- ¹⁸Y.-H. Lu, C.-W. Yang, C.-K. Fang, H.-C. Ko, and I.-S. Hwang, *Sci. Rep.* **4**, 7189 (2014).
- ¹⁹T. Nishiyama, Y. Yamada, T. Ikuta, K. Takahashi, and Y. Takata, *Langmuir* **31**, 982 (2015).
- ²⁰X. H. Zhang, N. Maeda, and J. Hu, *J. Phys. Chem. B* **112**, 13671 (2008).
- ²¹X. H. Zhang, X. Zhang, J. Sun, Z. Zhang, G. Li, H. Fang, X. Xiao, X. Zeng, and J. Hu, *Langmuir* **23**, 1778 (2007).
- ²²J. R. T. Seddon, O. Bliznyuk, E. S. Kooij, B. Poelsema, H. J. W. Zandvliet, and D. Lohse, *Langmuir* **26**, 9640 (2010).
- ²³X. Zhang and N. Maeda, *J. Phys. Chem. C* **115**, 736 (2011).
- ²⁴W. A. Ducker, *Langmuir* **25**, 8907 (2009).
- ²⁵M. P. Brenner and D. Lohse, *Phys. Rev. Lett.* **101**, 214505 (2008).
- ²⁶K. Yasui, T. Tuziuti, W. Kanematsu, and K. Kato, *Phys. Rev. E* **91**, 033008 (2015).
- ²⁷J. H. Weijs and D. Lohse, *Phys. Rev. Lett.* **110**, 054501 (2013).
- ²⁸D. Lohse and X. Zhang, *Phys. Rev. E* **91**, 031003 (2015).
- ²⁹B. Dollet and D. Lohse, *Langmuir* **32**, 11335 (2016).
- ³⁰Y. Gao, J. Li, H. C. Shum, and H. Chen, *Langmuir* **32**, 4815 (2016).
- ³¹J. L. Parker, P. M. Claesson, and P. Attard, *J. Phys. Chem.* **98**, 8468 (1994).
- ³²H. Teshima, K. Takahashi, Y. Takata, and T. Nishiyama, *J. Appl. Phys.* **123**, 054303 (2018).
- ³³W. Walczyk, P. M. Schön, and H. Schönherr, *J. Phys. Condens. Matter* **25**, 184005 (2013).
- ³⁴C.-W. Yang, Y.-H. Lu, and I.-S. Hwang, *J. Phys. Condens. Matter* **25**, 184010 (2013).
- ³⁵B. Zhao, Y. Song, S. Wang, B. Dai, L. Zhang, Y. Dong, J. Lü, and J. Hu, *Soft Matter* **9**, 8837 (2013).
- ³⁶Y.-H. Lu, C.-W. Yang, and I.-S. Hwang, *Appl. Surf. Sci.* **304**, 56 (2014).
- ³⁷Y.-H. Lu, C.-W. Yang, and I.-S. Hwang, *Langmuir* **28**, 12691 (2012).
- ³⁸J. E. Sader, J. W. M. Chon, and P. Mulvaney, *Rev. Sci. Instrum.* **70**, 3967 (1999).
- ³⁹R. P. Berkelaar, E. Dietrich, G. A. M. Kip, E. S. Kooij, H. J. W. Zandvliet, and D. Lohse, *Soft Matter* **10**, 4947 (2014).
- ⁴⁰F. J. Giessibl, H. Bielefeldt, S. Hembacher, and J. Mannhart, *Appl. Surf. Sci.* **140**, 352 (1999).
- ⁴¹Y. Hosokawa, T. Ichii, K. Kobayashi, K. Matsushige, and H. Yamada, *Jpn. J. Appl. Phys., Part 1* **47**, 6125 (2008).
- ⁴²J. E. Sader and S. P. Jarvis, *Appl. Phys. Lett.* **84**, 1801 (2004).
- ⁴³J. R. T. Seddon, E. S. Kooij, B. Poelsema, H. J. W. Zandvliet, and D. Lohse, *Phys. Rev. Lett.* **106**, 056101 (2011).